

## ERIS: An emittance reconstruction application for Linac3

Emmanouil Trachanas<sup>1,2,\*</sup>, Georgios Voulgarakis<sup>1</sup>, Veliko Atanasov Dimov<sup>1</sup>, Alessandra Lombardi<sup>1</sup>, Giulia Bellodi<sup>1</sup> and Evangelos Gazis<sup>1,2</sup>

<sup>1</sup>Conseil Européen pour la Recherche Nucléaire (CERN)

<sup>2</sup>National Technical University of Athens (NTUA)

Received 10 April 2019; Accepted 20 December 2021

### Abstract

Inspector and Inspector Services framework are innovative developer tools, designed at CERN and used for the design of control applications at the CERN accelerator complex. This paper presents the use of this framework in the implementation of an application that permits fast emittance reconstruction from profile measurements at Linac3 using the quadrupole variation method. The theoretical background is presented along with measurements, simulations, error analysis and technical characteristics of the application and software platform.

*Keywords:* CERN, Linac3, Quadrupole variation method, control and measurement application, Inspector software

### 1. Introduction

Linac3 is the first stage of the heavy ion acceleration at CERN (Conseil européen pour la recherche nucléaire). It accelerates different ion species like Lead, Argon and Xenon for the Large Hadron Collider (LHC) and for fixed target experiments [1]. The ion beams are produced with an electron cyclotron resonance (ECR) ion source at an initial energy of 2.5 keV/u. The beam then enters the Low Energy Beam Transport (LEBT) and then the RFQ with an exit energy of 250 keV/u, followed by an Interdigital-H Drift Tube Linear Accelerator (IH-DTL) which further accelerates the beam up to the Linac3 output energy of 4.2 MeV/u [1]. The ion source and the LEBT section of Linac3 are shown in Fig 1. The unwanted charge states from the source are filtered with a 135° spectrometer system. The selected beam is then matched to the RFQ with three electromagnetic quadrupoles and a solenoid magnet. The cylindrical symmetry of the beam is restored with the quadrupole magnets and the final focusing is performed with the solenoid.

A secondary electron emission (SEM) grid and a beam current transformer (BCT) are used to monitor the beam properties after the electromagnetic quadrupoles. During recent years, in the framework of the LHC Ion Injector Upgrade program, several activities have been carried out to improve the ion source and Linac3 performance [2]. The detailed study of the ion source extraction region and the LEBT followed by few hardware changes resulted in increase in the beam intensity at the RFQ entrance by 20 % [1]–[4]. Afterwards, a thorough campaign of beam measurements and simulations was carried out to characterize the beam parameters in the LEBT and determine the settings of the magnetic elements for the matching of the beam to the RFQ. Characterization of the transverse beam emittance in the LEBT is crucial for the beam matching to the RFQ hence the performance of the whole linac.

Henceforth, the motivation of this study was to design and develop a control room application for automatized emittance measurement before the quadrupole triplet of LEBT (see Fig.1 point R) using measurements from the SEM grid (see Fig.1-point M) and in-house software framework to accelerate and systematize the process of beam data measurement and analysis. This paper is divided in 5 sections. Section 2 describes the algorithmic implemented method for emittance reconstruction: the quadrupole variation, a method well established and studied (see Refs. [5]–[8]).

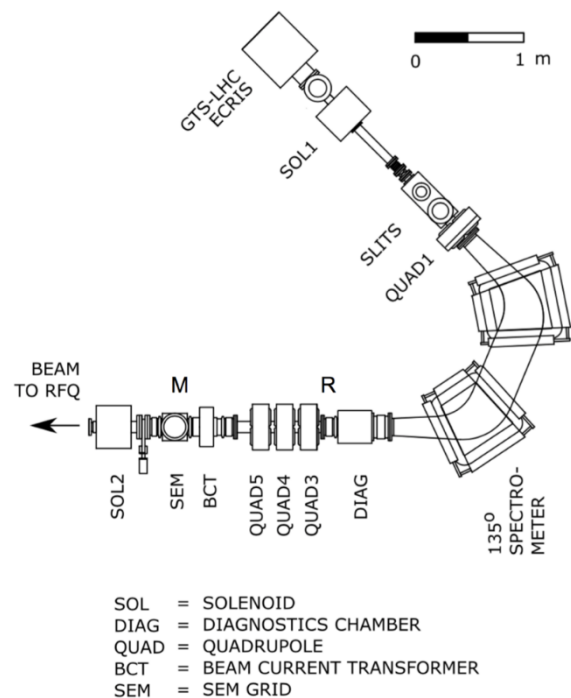


**Fig. 1.** Linac3 technical design with the exact place of the emittance reconstruction (R) and measurement point (M) inside LEBT after the Ion Source [1].

\*E-mail address: Emmanouil.Trachanas@ess.eu

ISSN: 1791-2377 © 2021 School of Science, IHU. All rights reserved.

doi:10.25103/jestr.146.01

Section 3 and 4 present the "virtual measurements" to validate the correct implementation of the method and investigate different factors that contribute to errors on the results. The whole project was accomplished taking advantage the accelerator control network of CERN and the special tools Inspector and Inspector Services for the design of control applications [11], which are outlined in section 4 along with the detailed description of ERIS application.

## 2. Measurement Set-up and the Method

Fig. 2 shows the section of the LEBT used for the emittance measurements. It is also shown in Fig. 1 between points R (reconstruction) and M (measurement). The measurement strategy is based on the well-established quadrupole variation method ([5]-[8]) where the beam matrix can be reconstructed at point R by measuring the beam size at point M by varying the settings of the quadrupole magnets between them.

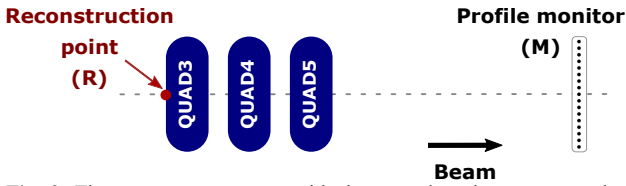


Fig. 2. The measurement setup with three quadrupole magnets and a profile monitor.

It was decided to use three quadrupole magnets (QUAD3: focusing, QUAD4: defocusing and QUAD5: focusing) for the emittance measurements for more flexibility on varying the beam size at the profile monitor and, simultaneously, have a better control of the beam in view of reducing the particle losses during the measurements. In addition, as the reconstruction point is upstream of all the elements used for the beam matching to the RFQ, the reconstructed beam parameters can directly be used as an input for matching studies.

If the motion in two transverse planes is uncoupled and the nonlinear forces (like space charge) are ignored, in each transverse plane, the beam matrix at the measurement and the reconstruction points are related to each other through the  $2 \times 2$  transfer matrix as shown in Eq. 1:

$$\sigma^M = R \sigma^R R^T \quad (1)$$

In Eq. 1 and throughout this paper, the superscripts R and M represent the reconstruction and measurement points, respectively, and  $R$  is the transfer matrix from the former to the latter. By performing beam profile measurements with different optics conditions, it is possible to construct a linear system and solve for the elements of  $\sigma^R$ . In principle, three measurements are sufficient to solve for three unknowns. However, having more measurements and using least square fitting method for solving the overdetermined system reduces the error in the reconstruction process [9]. It is possible to write a system of  $n$  equations in matrix formalism as in Eq. 2

$$\Sigma^M = A \Sigma^R \quad (2)$$

In Equation 2,  $\Sigma^M$  and  $\Sigma^R$  are vectors containing the information from the measurements and the unknowns, respectively (see Eq. 3). Likewise,  $A$  is a  $n \times 3$  matrix constructed using the elements of transfer matrices from each measurement (see Eq. 4)

$$\Sigma^M = \begin{pmatrix} \sigma_{11}^M(1) \\ \sigma_{11}^M(2) \\ \vdots \\ \sigma_{11}^M(n) \end{pmatrix}, \quad \Sigma^R = \begin{pmatrix} \sigma_{11}^R \\ \sigma_{12}^R \\ \vdots \\ \sigma_{22}^R \end{pmatrix} \quad (3)$$

$$A = \begin{pmatrix} R_{11}^2(1) & 2R_{11}R_{12}(1) & R_{12}^2(1) \\ R_{11}^2(2) & 2R_{11}R_{12}(2) & R_{12}^2(2) \\ \vdots & \vdots & \vdots \\ R_{11}^2(n) & 2R_{11}R_{12}(n) & R_{12}^2(n) \end{pmatrix} \quad (4)$$

Eq. 2 can be solved using least squares fitting method as shown in Eq. 5:

$$\Sigma^R = (A^T A)^{-1} A^T \Sigma^M \quad (5)$$

Once the vector  $\Sigma^R$  is defined,  $\sigma^R$  matrix can be reconstructed and unnormalized rms emittance and the Twiss parameters can be calculated. If only one quadrupole was varied for the measurement, the reconstruction result and the measured rms beam sizes (or square of the rms beam size) can be visualized in the same plot by simulating the measurements using Eq. 1 and the reconstructed beam matrix  $\sigma^R$ . Fig. 3 shows an example of a reconstruction in both horizontal and vertical planes using the data from virtual measurements (see Section 3) where QUAD5 was varied. The plots on the right compare the measured rms beam size and the beam size obtained by simulating the  $\sigma^R$  to point M by varying the quadrupole with a smaller step size than the one in the measurement. In the figures, the simulated curve can be considered as the fit to the measured discrete data. Another way to compare the measurement data and the reconstruction result is to project the measured rms beam sizes from M onto the phase space at R and plot the projections along with the reconstructed rms ellipse. Eq. 6 where the symbol  $i$  corresponds to the  $i^{th}$  measurement ( $1 \leq i \leq n$ ) and  $R_{11}$ ,  $R_{12}$  are elements of the transfer matrix; shows how a position ( $x$ ) at M (with unknown divergence,  $x'$ ) projects onto the phase space at R.

$$x^M(i) = R_{11}(i)x^R(i) + R_{12}(i)x'^R(i) \quad (6)$$

The measured rms beam size,  $x_{rms}$ , represents the maximum extend of the rms ellipse in position axis at point M. Therefore, projection of  $x_{rms}$  and  $-x_{rms}$  gives a couple of parallel lines which in perfect conditions are tangent to the rms ellipse in the phase space at point R. The plots on the left in Fig. 3 show the reconstructed rms ellipses and the projected lines plotted together. As there are no errors introduced, the projected lines are tangent to the reconstructed rms ellipses. If errors are present in the measurement, the projected lines may intersect the rms ellipse at two points or they may not intersect at all.

## 3. Virtual Measurements

The method and the implementation of formulas presented in Section 2 were validated through virtual measurements. First, multiparticle beam dynamics simulations were performed using Travel software and its graphical user interface PATH Manager [10] to scan a quadrupole and extract the beam size at point M. Then, using the method presented in Section 2 and the simulated beam size, the emittance and the Twiss parameters were calculated at point R. Finally, the values obtained from the calculations were compared with the reference ones used in the simulations to estimate the error.

For the simulations, a Lead ( $Pb^{29+}$ ) beam with 50000 macroparticles was used. The reference beam properties at point R are given in Tab. 1. The reference beam was generated

with zero energy spread and the simulations were performed without introducing any space-charge effects.

**Table 1.** Reference beam properties at point R used for virtual measurements.

Property	Horizontal	Vertical
$\epsilon_{rms, norm}$ (pi.mm.mrad)	0.2	0.2
$\alpha$	-6.77	-2.89
$\beta$ (mm/mrad)	2.14	0.85

For the virtual measurements, QUAD3 and QUAD4 were set to 1.4 and 1.9 T/m, respectively, while QUAD5 was varied from 1 to 1.35 T/m with a step size of 0.05 T/m. Fig. 3 shows the result of the virtual measurements for the two transverse planes. In both planes, the error in measured emittance and Twiss parameters are below  $10^{-8}$ %.

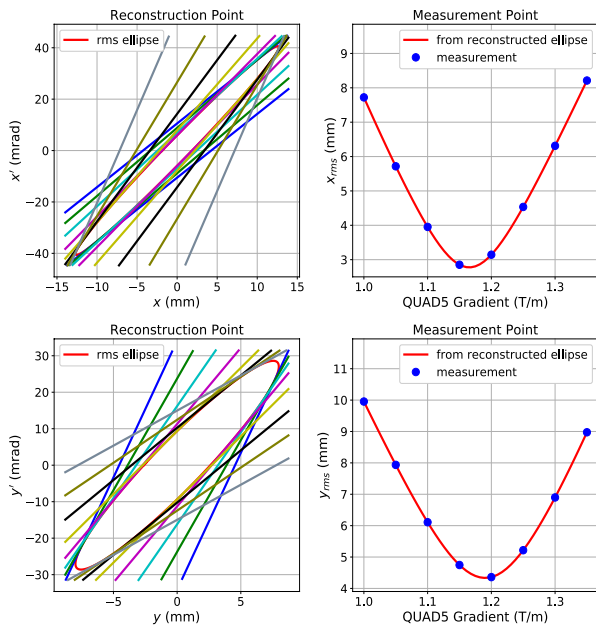


**Fig. 3.** Result of virtual measurement: (Left) reconstructed rms emittance ellipse and the projections of measured rms beam sizes at the reconstruction point, (Right) measured rms beam sizes and beam size resulting from tracking of the reconstructed rms emittance ellipse.

#### 4. Error Investigation

In the previous section it was shown that, under ideal conditions, the error in parameters of the reconstructed rms ellipse is negligible. The scope of this section is to investigate the possible errors introduced by several factors like, error in measured beam size, error in quadrupole gradients and the beam current. The effect of beam current was studied by gradually increasing it and performing a single virtual measurement for each case. However, the effect of error in measured beam size and quadrupole gradients was studied statistically by increasing the error level and performing 10000 virtual measurements for each level. The details and result of each case are given in the following sections. As the results in the two transverse planes are similar, for the sake of simplicity, only the result of horizontal plane will be presented in this paper.

##### 4.1. Estimation of Errors in Beam Size Measurements

In each transverse plane, the Linac3 LEBT SEM grid covers a total width of 82 mm with a wire spacing of 3.4 mm [12]. In order to estimate the beam size measurement error, which

results solely from the physical properties of the SEM grid, its geometry was simulated using beams with Gaussian distribution having different rms beam sizes (with 1000000 macroparticles). Each beam was moved across the SEM grid by an amount equal to the wire spacing in 1000 steps. At each step, the rms beam size was calculated considering the wire positions and the number of particles falling on each wire. The calculated rms beam size was then compared with the reference beam size to estimate the error. Fig. 4 shows the distribution of expected errors in beam size measurements for a reference beam size of 8.0 mm. As it can be seen, the errors form a Gaussian like distribution (regardless of the reference beam size).

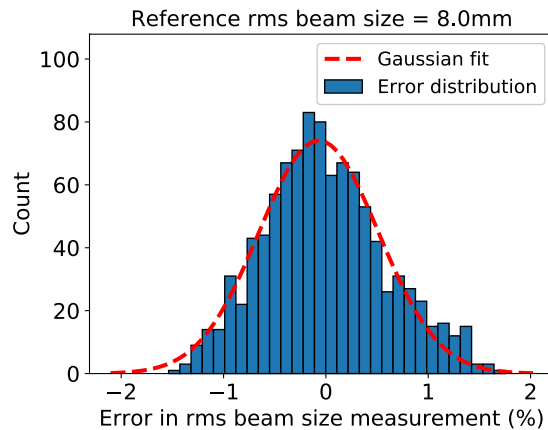


**Fig. 4.** Distribution of rms beam size measurement errors for a reference rms beam size of 8.0 mm.

Fig. 5 shows the summary of the distribution of errors in beam size measurements for beams having rms sizes between 3 mm and 13 mm. Outside of this range the SEM grid is not suitable due to wire spacing (for small beam sizes) or the total width (for large beam sizes). As it can be seen in the figure, regardless of the reference beam size, the standard deviation of the error distribution is always around 0.6 % of the reference rms beam size.

The study described above was repeated using beam with uniform distribution in x-y plane. The calculations showed that for uniform beams the standard deviation of the error distribution could go up to 1.0 % of the reference rms beam size.

##### 4.2 Effect of Beam Size Measurement Error on Reconstructed Emittance

It was shown in Section 4.1 that the physical properties of the SEM grid can introduce certain error depending on the relative position of the beam and the SEM grid. In addition, electronic noise and analysis of the measured beam profile (for instance choice of threshold or baseline) can introduce further error in the calculation of rms beam size. In order to estimate the effect of the beam size measurement error on the

reconstructed emittance, the virtual measurements described in Section 3 were repeated by introducing random errors on each measured beam size. Following the results presented in Section 4.1, the errors were generated independently for each measured point with Gaussian distribution having standard deviation equal to certain percentage ( $p$ ) of the corresponding reference rms beam size as shown in Eq. 7 where symbol  $i$  represents the measurement number as in Eq 6. Moreover, to observe the trend of the distribution of errors in reconstructed ellipse parameters  $p$ . was increased gradually and 10000 virtual measurements were performed for each error level.

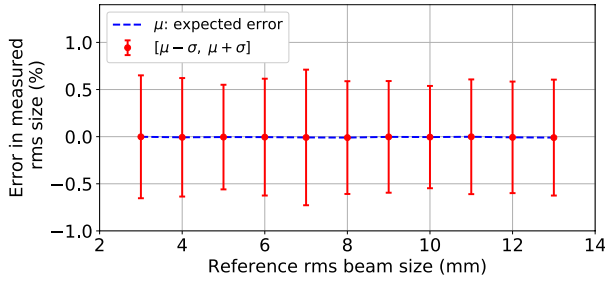


Fig. 5. Summary of the beam size measurement errors. Blue line represents the mean of the error distributions and the error bars represent the standard deviation of the distributions.

$$\sigma_{err}(i) = px_{rms}(i) \quad (7)$$

Fig. 6 shows the resulting error distribution for emittance for  $p=0.6\%$ . Just like emittance, the distribution of errors in alpha and beta also form a Gaussian distribution.

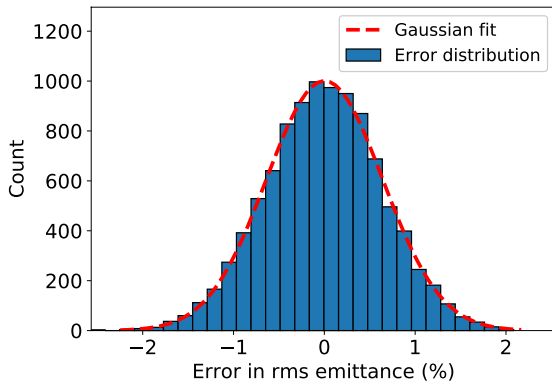


Fig. 6. The resulting distribution of errors for emittance when  $p=0.6\%$ .

Fig. 7 shows the summary of the errors in reconstructed ellipse parameters with the increasing error in the beam size measurements. As it can be seen in the figure, the expected error for alpha, beta or emittance is almost unchanged however the standard deviation of the distribution of errors grows linearly as  $p$  increases.

Fig. 8 (left) shows 2D binning of errors for alpha and beta for  $p=0.6\%$ . As it can be seen in the figure, there is a clear correlation between the errors in alpha and beta. This is mostly due to the reconstruction process. Because emittance is inversely proportional to alpha and beta, error in alpha and beta is coupled with the error in emittance. This is clearly visible in Fig. 8 (right) where the coupling is shown in a 2D color map.

## 4.2. Effect of Quadrupole Gradient Error on Reconstructed Emittance

The quadrupole variation method uses transfer matrices to reconstruct the rms ellipse parameters. Therefore, precise knowledge of the quadrupole gradients is important for accurate results. For instance, wrong calibration of the quadrupole magnets or jitter of the magnet currents during the measurements would contribute to errors in reconstructed emittance and Twiss parameters. The impact of quadrupole gradient errors on reconstructed emittance was studied by performing virtual measurements (described in Section 3) with random errors on each of the three quadrupole gradients. The error ( $err_G$ ) was increased gradually from 0.2% to 1.6% and for each level 10000 virtual measurements were performed by generating uniform errors between  $-err_G$  and  $err_G$  independently for each quadrupole. The resulting distributions of error in rms emittance and Twiss parameters are Gaussian as in the case of Section 4.2. Fig. 9 summarizes the properties of the distribution of errors in the rms ellipse parameters.

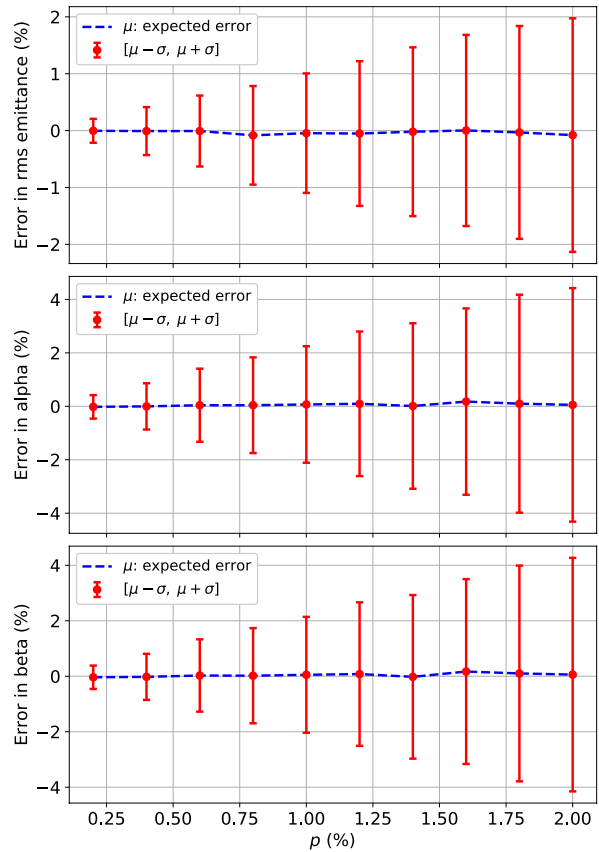


Fig. 7. Summary of errors in reconstructed ellipse parameters for different levels of beam size measurement errors. Blue line represents the mean and error bars represent the standard deviation of the distributions.

## 4.3. Effect of Space Charge on Reconstructed Emittance

With the upgrade of Linac3 source extraction in 2016, the lead beam current at the RFQ input was increased from 170μA to 210μA [2]. Effect of the beam current on the reconstructed ellipse parameters was calculated via virtual measurements by increasing the beam current for the multi-particle tracking with Travel. Fig. 10 shows how the reconstructed emittance and Twiss parameters are affected by beam current. As it can be seen in the figure, the error in all the parameters increase linearly with the beam current. For a beam current of 210μA, the expected error in rms emittance is around 8%

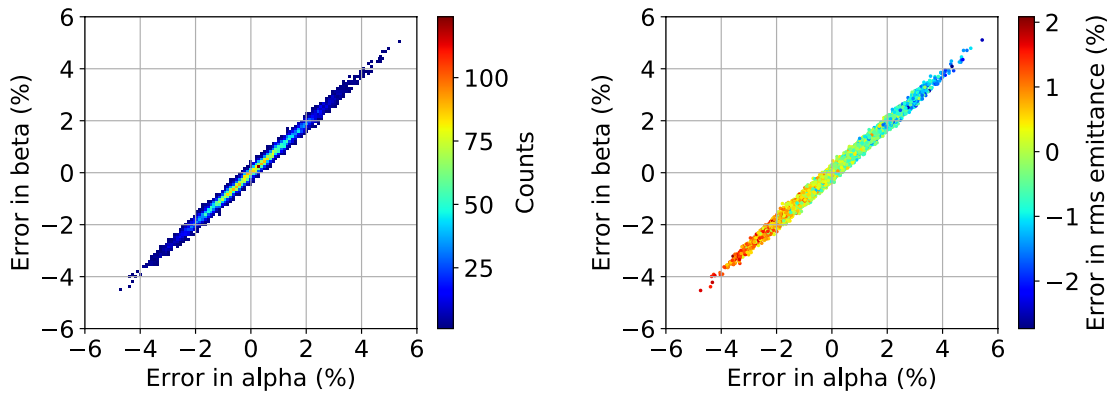


Fig. 8. (left) 2D binning of errors in alpha and beta, (right) coupling of errors in alpha and beta with error in emittance for  $p=0.6\%$ .

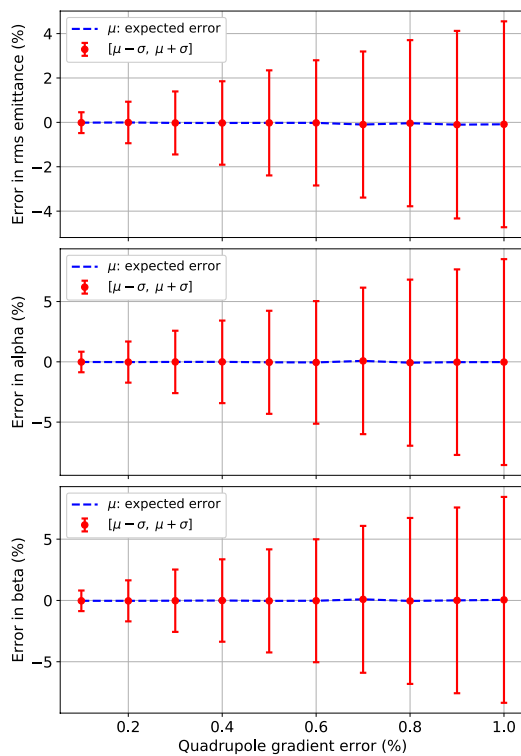


Fig. 9. Summary of errors in reconstructed ellipse parameters for different levels of quadrupole gradient errors. Blue line represents the mean and error bars represent the standard deviation of the distributions.

## 5. Control Application Development

### 5.1. Introduction

This section probes the technical implementation and software integration of the theoretical analysis of previous sections. The presentation of the application starts with the description of the Inspector and Inspector Services framework used widely at CERN and proceeds to a detailed description of the ERIS (Emittance Reconstruction Integrated Software) and its functionality. In order to control the large

number of complex devices and machines CERN has a three layer architecture (Fig. 11) that controls and monitors the data transfer from the low-level circuit logic until the level of the CERN Control Center (CCC):

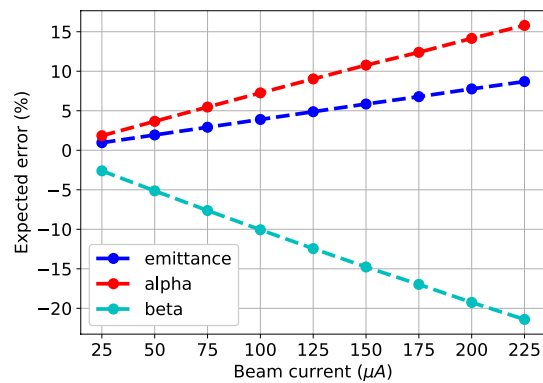


Fig. 10. Error in the reconstructed ellipse parameters with increasing beam current.

**1.Device Layer:** The first and basic layer where all the devices are located. The devices communicate with the upper next layer in hierarchy using the FESA framework (Front End Software Architecture). A physical device is assigned to a rack and connected with a computer using the FESA framework.

**2.Middle Layer:** The front-end computer transfers the device data to the Middle Layer for processing. Furthermore, it processes all the operator commands and stores the settings sent to the devices. It is the layer that effectively connects the physical devices with the operators. It communicates with the front-end computer using JAPC (Java API-Application Programming Interface for Parameter Control). The middle layer transfers the data given from the high-level control applications to low-level settings for the devices.

**3. Application Layer:** At this layer all high-level applications used by the operators are contained. With these applications the operator can control a device, make measurements, and depict vital device information and settings, exchanging data with the Middle Layer [11].

Inspector is a graphical framework that permits the design of user interfaces for the control of a device inside CERN grid. Inspector facilitates the control of a device and the depiction of the vital operational machine information. The framework is characterized by the term **data-driven** allowing user to select the value that he/she wants to visualize or change and drag-and-drop it to the panel in accordance with the data type. It offers a vast spectrum of possibilities permitting to perform complex control of the accelerator chain devices in a simple way. Inspector has a client-server architecture and uses a proxy to communicate and pass data

to the available corresponding servers. The flexibility and the adaptability of this framework offers the possibility to create new servers depending on the needs and transfer the data to other ones in case of server failure. There are three kinds of servers: **data** for direct data, **synthetic** for real time evaluation of data and **logging & alarm** servers (see Fig. 12). The rapid prototyping of this framework permits the handling of applications and algorithms developed in different environments and programming languages with little effort [11].

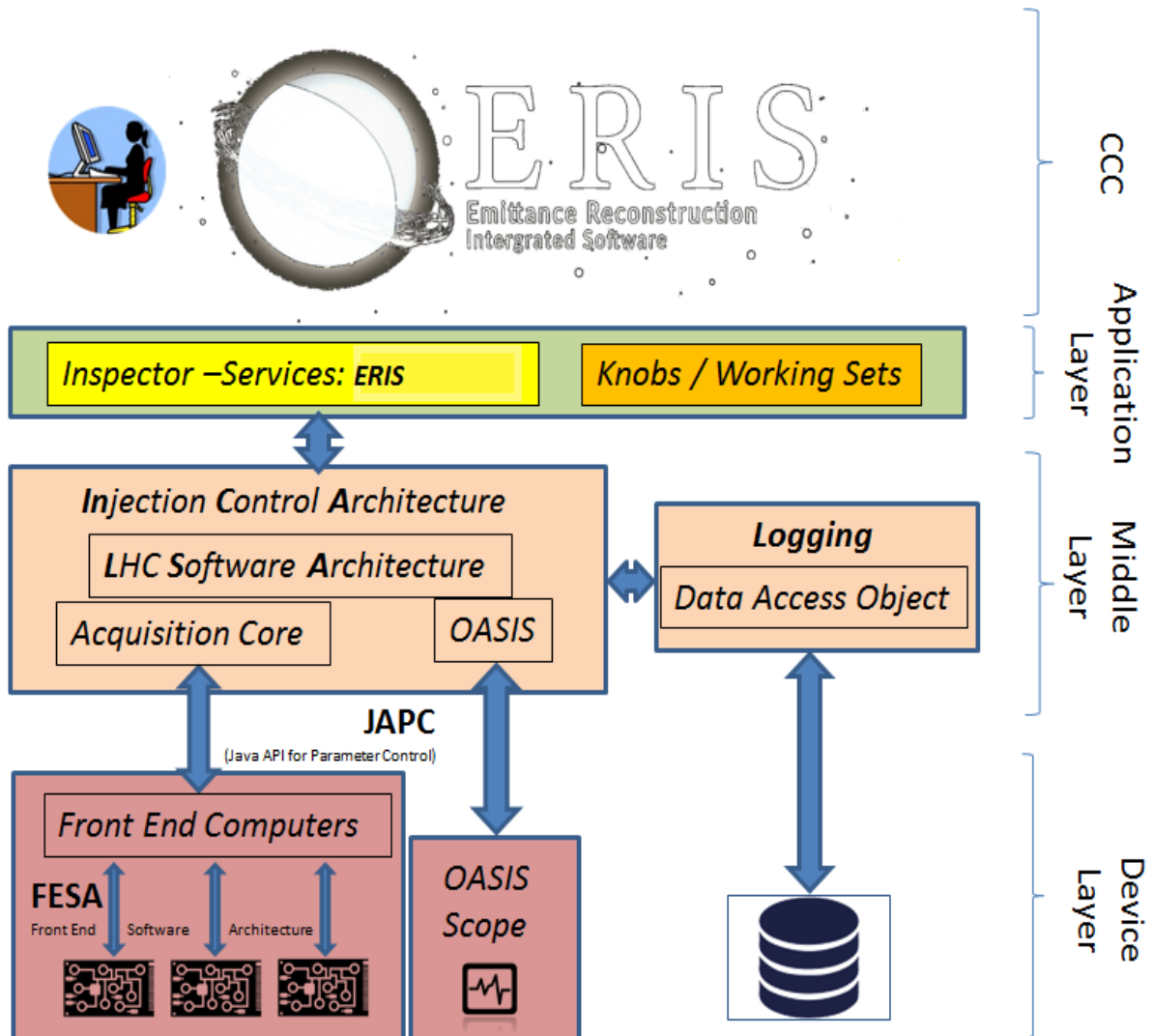


Fig. 11. CERN data transfer layer Architecture [11].

### 5.3. Inspector Services

Inspector allows the operator to monitor a device and perform calculations and measurements although, more complicated procedures and complex algorithms can be performed through the Inspector services extension. A service is a code, which implements and executes an algorithm. The underlying implementation of the Inspector Services framework is done in Java; thus, a service can be designed using any Java development interactive development environment (IDE- such as Eclipse or NetBeans). After the design process the Service is stored to Service Code Repository and installed on

dedicated servers (Service Servers) from where it can be deployed and executed. Inspector panels and designed user interfaces allow access to the Service Code Repositories and the dedicated server from any computer. The philosophy of Inspector and Inspector Services is centralized installation, instantiation and execution of the services and decentralized client control, establishing a client-server interaction. There are two kinds of Service servers: **Services Repository Servers** which contain the source codes of the services and **Services Execution Servers** (see Fig. 12) [11].

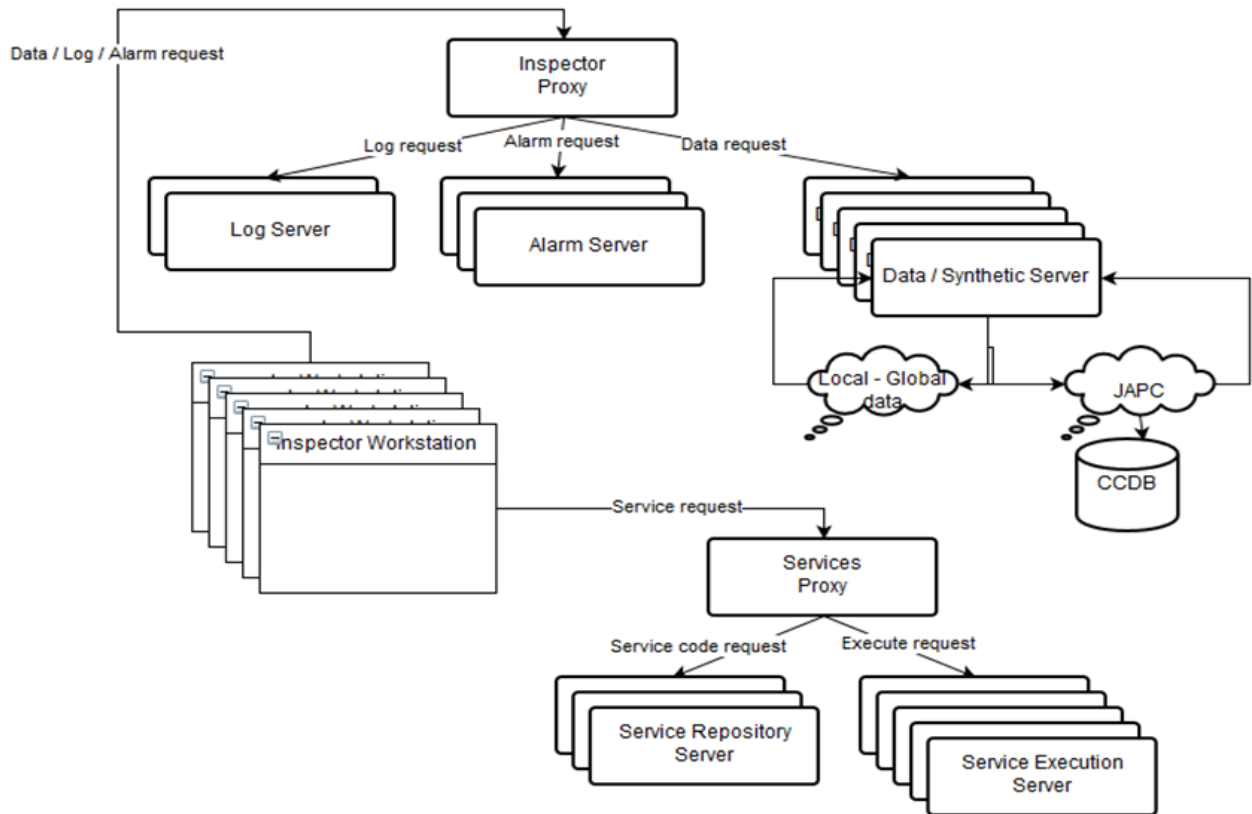


Fig. 12. Schema of Inspector and Inspector Services servers [11].

## 5.4. ERIS

### 5.4.1. Graphical User Interface and Functionality

ERIS: (Emittance Reconstruction Integrated Software) is an application that automatizes the emittance reconstruction at Linac3. The application which is deployed at the Linac3 control room allows user to set the values of the quadrupole magnets (see Fig. 1), takes the measurement profiles of the SEM grid and reconstructs the emittance (" Reconstruction

Point" on Fig. 2) in real time. The GUI of the application as launched from the control room is shown in Fig. 13.

At the foreground the blueprint design of the Linac3 LEPT showing the quadrupole triplet, the drifts, the deflectors and the SEMgrid. By double-clicking on each of the element's vital information regarding the acquisition values of quadrupoles, the deflectors' state and the SEMgrid motor position are displayed. The GUI is completed by the control buttons of the application on the left side and the plotting section on the right.

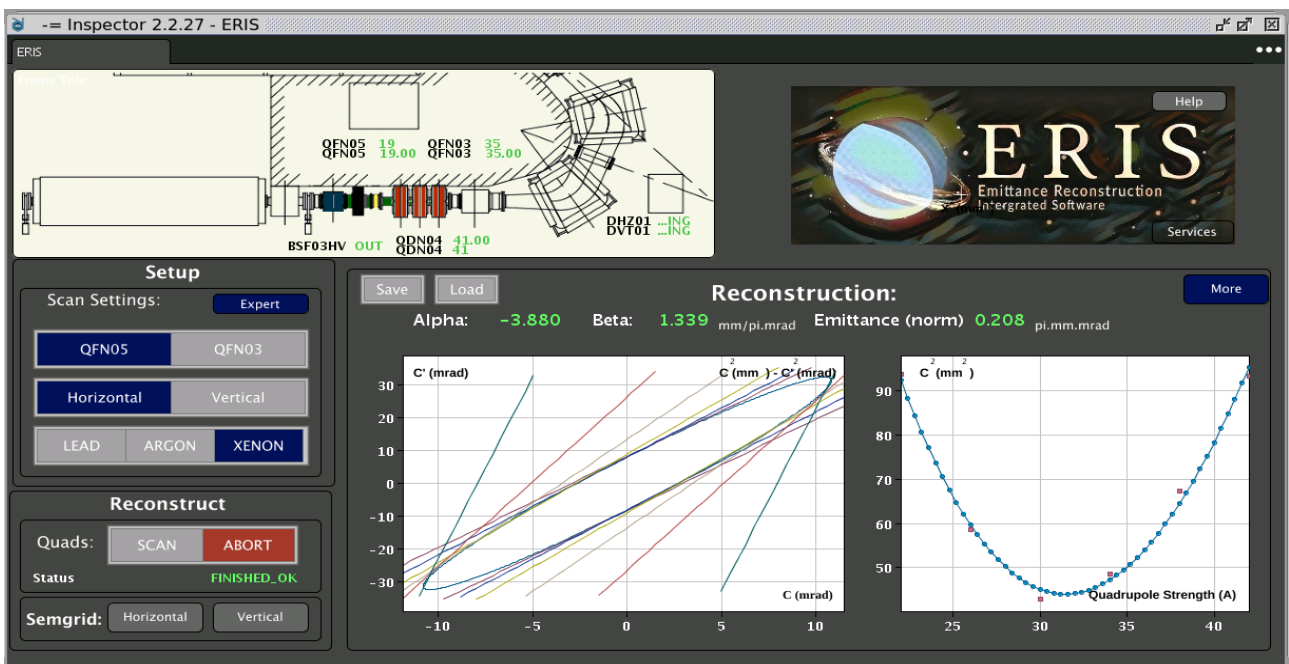


Fig. 13. Graphical User Interface of ERIS.

The plotting section shows the reconstruction results and the  $\alpha$ ,  $\beta$  and normalized emittance  $\epsilon$  only for the current plane. Horizontal and vertical reconstruction results appear together by clicking on the button "More" (see Fig. 15). The operator, to monitor the correct instantiation and function of the project services has to press the "Services" button inside the ERIS logo area; a log panel appears with details for the correct instantiation of application services. The application works with Lead  $29^+$ (Pb  $29^+$ ), Argon (Ar) and Xenon (Xe).

#### 5.4.2. Measurement Process and Data Acquisition

The first step of the algorithm is to choose a plane for the reconstruction (horizontal or vertical) the kind of particle and the quadrupole of the triplet to be scanned (the current of the first or last quadrupole is scanned and the rest have constant settings). At this point the front-end operator has two options: either to choose from a few sets of predefined settings for the

three quadrupoles or click on the "Expert mode" button and enter them manually by hand or via a stored file.

Moreover, the expert mode contains the time part of the pulse that is captured by the SEMgrid. By default, the program uses the first 200 $\mu$ s of the beam pulse (50 first gates-gates are 4 $\mu$ s separated) for calculations but the operator can modify it from the expert mode, leading to automatic recalculation with the desired gates. The application stores the SEMgrid data for every gate for every wire for the total of six measurements. Then the signals are averaged on the gates to extract the profiles on Fig. 14. The operator has the possibility to process the obtained profiles with the exclusion of certain wires with the definition of a certain area by clicking the middle mouse button and dragging on the measured profiles enabling to clean the noise in the tails of the profiles. At each processing step the results on the plotting windows are refreshed.

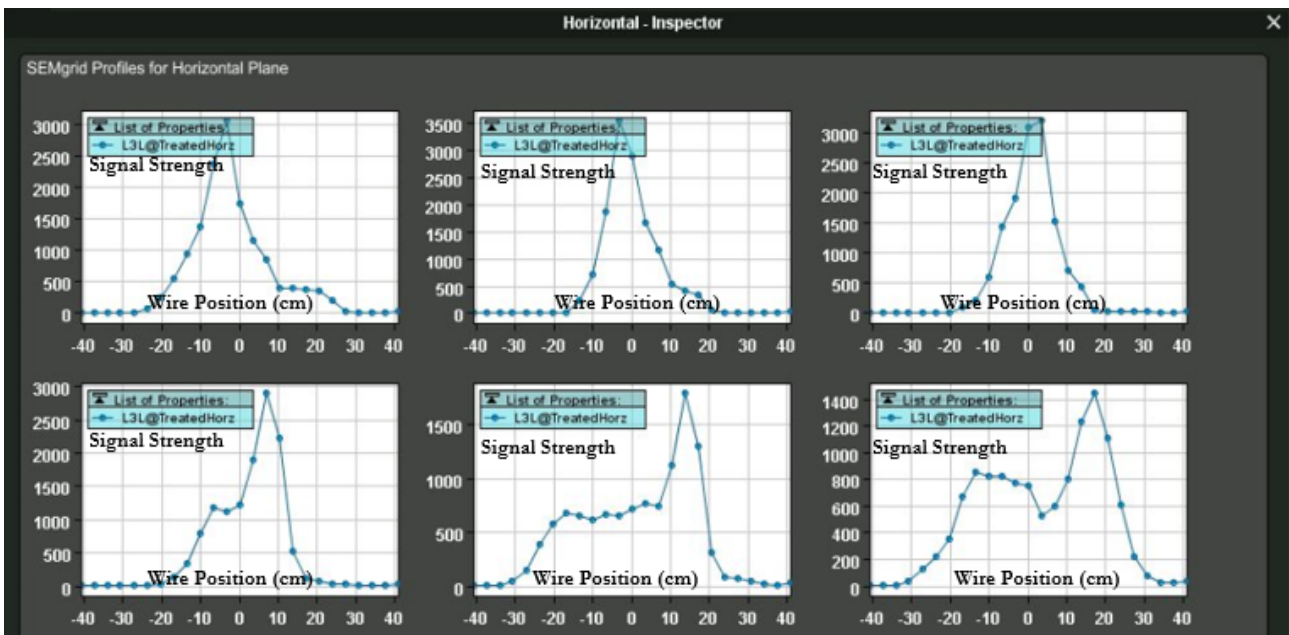


Fig. 14. Horizontal Profile Measurements from ERIS testing.

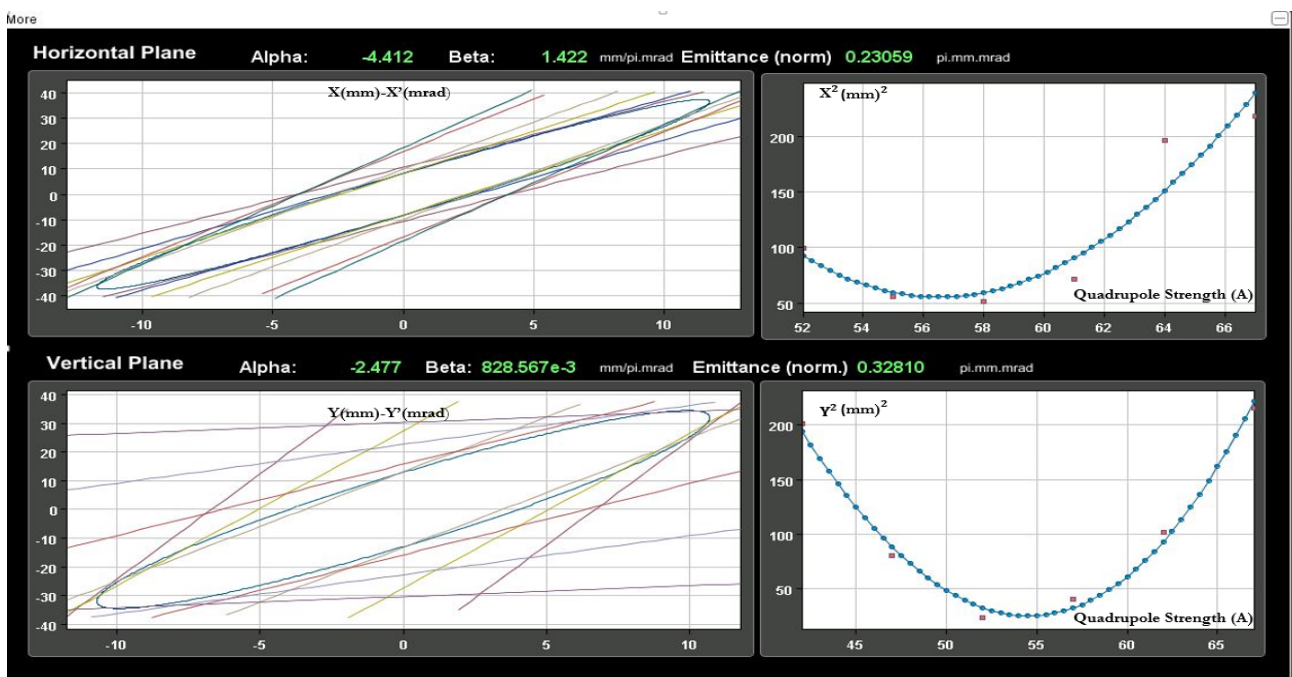


Fig. 15. Inside the "More" button with the reconstruction results on both planes.

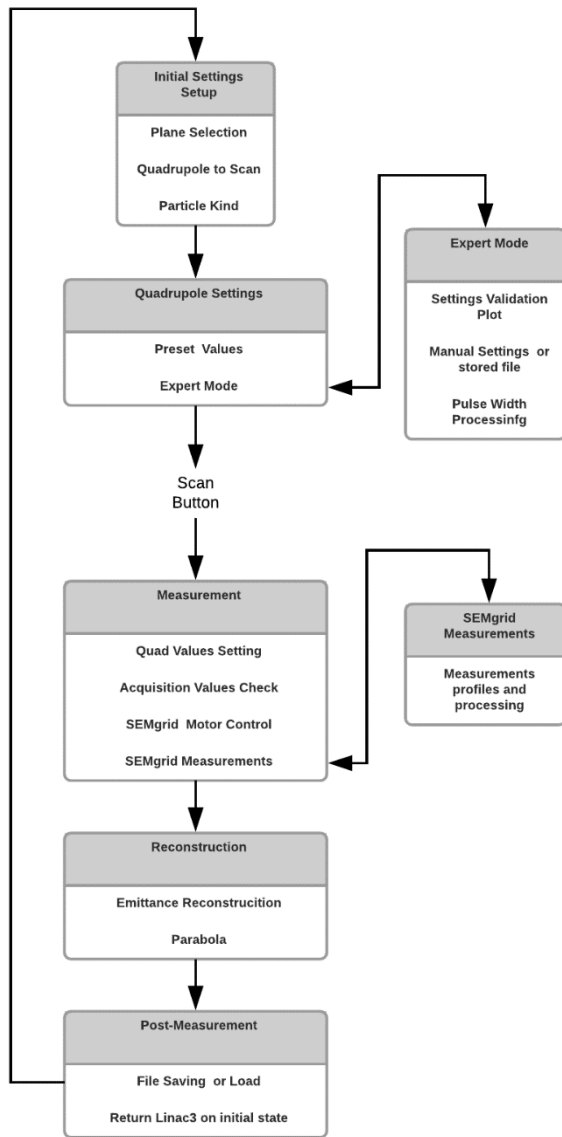


Fig. 16. ERIS Algorithm Flowchart and Technical aspects.

The detailed algorithm flowchart is shown below at Fig.16. With the click on the "SCAN" button the chosen values are set to the quadrupoles, the SEMgrid motor moves the SEM grid inside the beam pipe, the deflectors are turned off and measurements are starting to appear inside the measurement profiles windows of the corresponding plane (see Fig.:14 for horizontal plane). The reconstructed emittance within the tangent parallel lines and comparison of the  $x_{rms}$  points with the  $X^2$  fit are shown in the main menu of the application along with the  $\alpha, \beta, \gamma$  and emittance values. After a measurement the machine is returned to its initial state (SEMgrid out, Deflectors' state: ON and quadrupoles on their initial values). By clicking on "Save" button the operator can save two files (for horizontal and vertical plane) with the SEMgrid Measurements, the Processed Measurements, the gates used for sampling and the used quadrupole values in the desired path. enabling the possibility to load the results and settings of a past measurement.

## 6. Conclusion

ERIS is a powerful, versatile and fast diagnostic tool for online transverse emittance measurements developed for Linac3 LEBT section. In the framework of the Large Hadron Collider (LHC) Injectors Upgrade (LIU) project, the 2017 Xe run of Linac3 was particularly focused on increasing the beam dynamics understanding of the machine, in view of possible upgrades. [12] summarizes the measurements and simulations performed on Linac3 during the 2017 Xe run where ERIS was used for fast, real time emittance reconstruction (Analytical Method) [12]. ERIS converted the exhausting procedure of manual scanning, data extraction and offline analysis that took a significant amount of time down to a few minutes process via a user-friendly interface that permits the operation even by non-experts.

This is an Open Access article distributed under the terms of the Creative Commons Attribution License.



## References

- Toivanen et al.-Simulation of the CERN GTS-LHC ECR ion source extraction system with Lead and Argon ion beams." (2014). - Proceedings of ECRIS-2014, Nizhny Novgorod, Russia.
- Bellodi, G.-Source and Linac3 Studies-Proceedings of the Injector MD Days 2017, Geneva, Switzerland, 23-24 March 2017,-CERN Proceedings, Vol. 2/2017. DOI: 10.23727/CERN-Proceedings-2017-002.113,
- V. Toivanen, G. Bellodi, V. Dimov, D. Kuchler, A. M. Lombardi, and M. Maintrot , -Upgrade of the beam extraction system of the GTS-LHC electron cyclotron resonance ion source at CERN-Review of Scientific Instruments 87, 02B912 (2016) <https://doi.org/10.1063/1.4933118>
- V. Toivanen, G. Bellodi, C. Fichera, D. Kehler, A.M. Lombardi, M. Maintrot, A. Michet, M. O'Neil, S. Sadovich, F. Wenander , O. Tervainen-Recent developments with the GTS-LHC ECR Ion Source At CERN-Proceedings of ECRIS 2016, Busan, Korea. DOI: 10.18429/JACoW-ECRIS2016-WEA001
- X. J. Wang, R. Malone, K. Batchelor and I. Ben-Zvi, "Automatic emittance measurement at the ATF," Proceedings of International Conference on Particle Accelerators, 1993, pp. 2486-2488 vol.3, DOI: 10.1109/PAC.1993.309364.
- Ross, M.C., Phinney, N., Quickfall, G., Shoaee, H., & Sheppard, J.C. (1987)- Automated emittance measurements in the SLC (SLAC-PUB--4278). United States
- A. Mostacci, M. Bellaveglia, E. Chiodroni, A. Cianchi, M. Ferrario, D. Filippetto, G. Gatti, and C. Ronsivalle- Chromatic effects in quadrupole scan emittance measurements - Physical Review Special Topics-Accelerators and Beams 15, 082802 (2012). DOI: 10.1103/PhysRevSTAB.15.082802
- A.T. Green, Y.M. Shin - Development of a Python-based emittance calculator at Fermilab Science & Technology (FAST) Facility- Proceedings of NAPAC 2016, Chicago, IL, USA
- P. H. Richter- Estimating Errors in Least-Squares Fitting - The Telecommunications and Data Acquisition Progress Report, TDA PR 42-122, April-June 1995, pp. 107-137
- A. Perrin, J. Amand, T. Mutze, J. Lallement, and S. Lanzzone-Travel User Manual (CERN, 2007)
- G. Voulgarakis, J. Lettry, S. Mattei, B. Lefort, and V. J. Correia Costa -Autopilot regulation for the Linac4 H<sup>-</sup> ion source-AIP Conference Proceedings 1869, 030012 (2017) <https://doi.org/10.1063/1.4995732>
- S. Benedetti, G. Bellodi, D. Kuchler and V. Toivanen - The 2017 Xe run at Linac3: measurements and beam dynamics simulations-Review of Scientific Instruments 89, 123301 (2018)- <https://doi.org/10.1063/1.5066086>